



## Orientation and temperature dependence of yielding and deformation behavior of a nickel-base single crystal superalloy

L.N. Wang<sup>a,b</sup>, Y. Liu<sup>a,b,\*</sup>, J.J. Yu<sup>a</sup>, Y. Xu<sup>a</sup>, X.F. Sun<sup>a</sup>,  
H.R. Guan<sup>a</sup>, Z.Q. Hu<sup>a</sup>

<sup>a</sup> Institute of Metal Research, Chinese Academy of Sciences, Shenyang, 110016, PR China

<sup>b</sup> Graduate School of Chinese Academy of Sciences, Beijing, 100039, PR China

### ARTICLE INFO

#### Article history:

Received 15 June 2008

Received in revised form 3 November 2008

Accepted 17 December 2008

#### Keywords:

Single crystal superalloy

Yield strength

Dislocations

$\gamma'$  Precipitate

### ABSTRACT

Single crystal nickel-base superalloy SRR99 with orientation near  $\langle 001 \rangle$ ,  $\langle 011 \rangle$  and  $\langle 111 \rangle$  were tension tested at the temperature range from 20 to 900 °C. The experimental results showed that yielding strength of SRR99 alloy was anisotropic at all tested temperatures. The deformation mechanism was characterized by the matrix dislocation propagating on octahedral slip systems and shearing of  $\gamma'$  particles by dislocation pairs, loops and superlattice stacking faults. Meanwhile, the cross-slip of screw dislocations within  $\gamma'$  was thought to account for the tensile anisotropy. Fracture behavior was investigated by optical microscopy (OM) and scanning electron microscopy (SEM). It is of interest to note that the fracture surfaces of the three orientated samples tested at intermediate temperature indicate shearing rupture characteristic along  $\{111\}$  crystal plane.

© 2009 Elsevier B.V. All rights reserved.

### 1. Introduction

Nickel-base single crystal superalloy strengthened by coherent precipitates of the  $L1_2$  long range ordered  $\gamma'$  phase has been widely used as blade materials in gas turbine engines and power plants. However, the crystallographic alignment is never perfectly solidified along  $\langle 001 \rangle$  orientation and with deviations up to  $10^\circ$ . In addition, the blades are usually subjected to complex stress states, which will induce the activation of different slip systems. In order to get better understanding of the orientation dependence of the tensile behaviors of single crystals, many tests were carried out on single crystal superalloys, which exhibited very complicated yielding behavior [1–6]. One feature is the presence of peak yield strength, which means that the yield strength and critical resolved shear stress (CRSS) of many alloys do not decrease monotonically when the temperature increases, instead it would have a peak point at a certain temperature. This peak temperature was reported for many alloys with different volume fraction and size of  $\gamma'$  particles [7–10]. Another characteristic feature is the orientation dependence of yield strength and CRSS in single crystal superalloys. In other words, even for the orientation exhibiting normal octahedral slip the yield stress have been found not to follow the Schmid's law as a function of tensile axis and also differ in tension and compression tests.

In order to explain the orientation dependence of the yield strength and tension/compression asymmetry, many models were developed based on the deformation microstructures. Takeuchi and Kuramoto first paid attention to the violation of Schmid's law in  $Ni_3Ga$  and presented a model based on the thermally activated cross-slip of  $1/2 \langle 110 \rangle \{111\}$  screw superpartial dislocations from  $\langle 111 \rangle$  onto the  $\langle 010 \rangle$  plane [11]. By taking account of the core structure of the superpartial dislocations and the anisotropic elastic interaction between the two superpartial dislocations, Pardar et al. and Yoo [12–14] modified the model proposed by Takeuchi. The relationship presented by Miner et al. provides a simple way for modeling the orientation and direction dependence of the CRSS for octahedral slip in the temperature range where cross-slip pinning controls the yielding behavior [2]. Osterle et al. discussed the fitting parameter for different slip systems in various alloys and yielded a good consistency with experimental results [15].

Although many works have provided abundant of information that was essential for the better understanding of deformation mechanisms and the causes of yielding anomalous behavior, the influence of the specific alloy microstructure and chemical composition on anisotropic tensile behavior is still not clear. Therefore mechanical testing for different alloy system is necessary in order to obtain the reliable parameters required for the yielding behavior simulation. In the present study, tensile behavior and deformation microstructure of SRR99 alloy, which contains a high volume fraction of  $\gamma'$  particles, was investigated over the temperature range from 20 to 900 °C.

\* Corresponding author.

E-mail address: [Ivan.liu1026@yahoo.com](mailto:Ivan.liu1026@yahoo.com) (Y. Liu).

**Table 1**  
Nominal chemical composition of SRR99 alloy (wt%).

Al	Ti	Cr	Co	Ta	W	C	Ni
5.5	2.2	8.5	5.0	2.8	9.5	0.015	Bal.

## 2. Experiment procedure

The material used in this study is SRR99 single crystal superalloy. The nominal chemical composition of this alloy (wt%) is given in Table 1. The  $\langle 001 \rangle$  single crystals were produced by the withdrawn processes with deviation no larger than  $6^\circ$ . And the  $\langle 011 \rangle$  and  $\langle 111 \rangle$  single crystals were grown on a pre-fabricated seed of the desired orientation. Crystallographic orientation of the cast bars were determined by X-ray diffraction. The bars within  $10^\circ$  were accepted for tensile tests. As-cast bars were solution treated at  $1300^\circ\text{C}$  for 4 hours, and then aged at  $1100^\circ\text{C}$  for 4 hours and at  $870^\circ\text{C}$  for 16 hours respectively. The process of heat treatment produced a precipitation of regular cuboidal  $\gamma'$  particles aligning along  $\langle 100 \rangle$  in the  $\gamma$  matrix. The size of  $\gamma'$  is about  $0.4\text{--}0.5\ \mu\text{m}$  and the volume fraction of  $\gamma'$  phase is about 70%.

Cylindrical specimens were mechanically machined with a diameter of 5 mm and a gauge length of 25 mm. The tensile tests were carried out at the temperatures range from 20 to  $900^\circ\text{C}$  using an AG-250KNE machine. The initial strain rate was  $3.3 \times 10^{-4}\ \text{s}^{-1}$ . At least two specimens were tested for each orientation. Optical microscopy and scanning electron microscopy were used to observe the slip traces. Thin foils for transmission electron microscopy (TEM) observation were cut from the sections both perpendicular to the loading axis and parallel to fracture surface. A TECNAI20 instrument operated at 200 kV was used.

## 3. Results and discussion

### 3.1. Yield strength and stress–strain curves

The experimental results show that the elastic modulus of SRR99 alloy is highest in  $\langle 111 \rangle$  direction and lowest in  $\langle 001 \rangle$  direction, as shown in Fig. 1, which is coincident with the previous study [16]. With the increase of temperature the value of elastic modulus exhibits an apparent decrease for all orientations. The yield strength at different temperatures is presented in Fig. 2. For

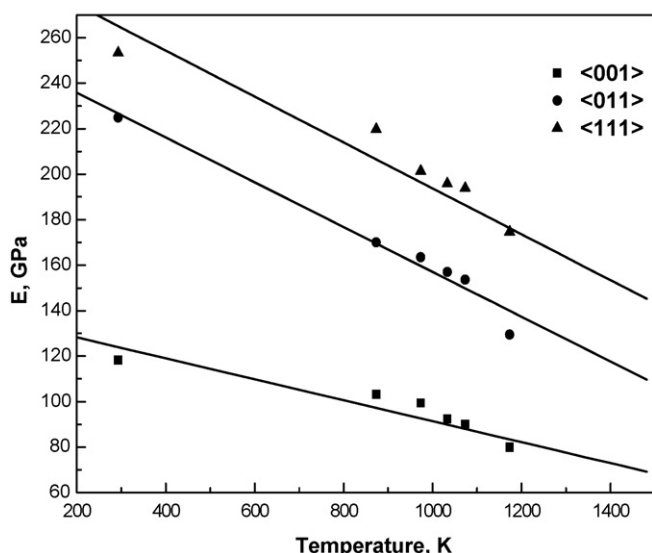


**Fig. 1.** Elastic modulus of different samples at tested temperatures.

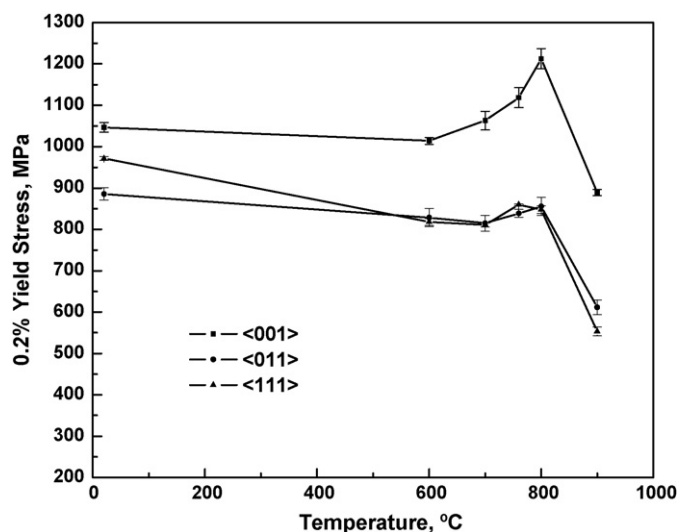


**Fig. 2.** Yield strength of SRR99 single crystal with different orientations.

specimens with  $\langle 001 \rangle$  orientation, the yield strength does not monotonically decrease with the rise of temperature. At the temperature of  $800^\circ\text{C}$ , it has a peak value of  $1215\ \text{MPa} \pm 25\ \text{MPa}$ . As for  $\langle 011 \rangle$  and  $\langle 111 \rangle$  crystals, no significant difference in yield strength is observed except that at room temperature. At the temperature regime from room temperature to  $700^\circ\text{C}$ , the yield strength of  $\langle 011 \rangle$  single crystal does not show a significant change. But at  $760^\circ\text{C}$ , it shows a slightly increase. At  $900^\circ\text{C}$ , decrease of yield strength for all specimens is quite pronounced. For all temperatures, the yield strength of  $\langle 001 \rangle$  specimens are considerably higher than that of the samples with the other two orientations.

Stress–strain curves at typical temperatures are shown in Fig. 3. At room temperature and at  $600^\circ\text{C}$ ,  $\langle 001 \rangle$  and  $\langle 011 \rangle$  specimens exhibited relatively low strain-hardening effect. However, for  $\langle 111 \rangle$  crystals, the flow stress increased dramatically with the rise of strain. One possible reason is that high density of dislocations in matrix channels are produced during the plastic deformation and the strong interaction among these dislocations would finally induce higher hardening effect. TEM observation in the following section also confirmed that  $\langle 111 \rangle$  samples had a higher dislocation density in matrix compared to that in  $\langle 001 \rangle$  and  $\langle 011 \rangle$  samples. When the temperature is above  $800^\circ\text{C}$ , the flow stress did not show a significant increase for the crystal with different orientations. This is likely caused by the fact that thermally-activated effect at high temperatures would avail the climb and cross-slip of mobile dislocations.

### 3.2. Dislocation microstructure and orientation dependence of CRSS

An overview of the dislocation microstructure in the  $\langle 001 \rangle$  crystal deformed at room temperature is shown in Fig. 4. It can be seen that plastic deformation takes place quite homogeneously and no slip bands is observed. The cubic morphology of the  $\gamma'$  phases was maintained at all tested temperatures. High density of dislocations is observed in matrix channels. Shearing of  $\gamma'$  by dislocation pairs and loops are also observed frequently. These dislocation pairs are generally coupled by an anti-phase boundary (APB). In addition, there is large amount of superlattice stacking faults (SSF) observed within  $\gamma'$  particles. Fig. 5 and Fig. 6 show the deformation microstructure of the  $\langle 001 \rangle$  specimen deformed at  $700^\circ\text{C}$ . It is noted that  $\gamma'$  particles are also sheared by superlattice stacking faults (SSFs) and dislocation pairs. The Burgers vector of the dislo-

Download English Version:

<https://daneshyari.com/en/article/1581108>

Download Persian Version:

<https://daneshyari.com/article/1581108>

[Daneshyari.com](https://daneshyari.com)